REGISTRATION OF RF ULTRASOUND DATA USING HYBRID LOCAL BINARY PATTERNS

T. Klein[1] *, M. Hansson*[2]*, A. Karamalis*[1]*, and N. Navab*[1]

[1]Computer Aided Medical Procedures (CAMP), Technische Universität München, Germany
[2]Malmö University, School of Technology, Sweden

ABSTRACT

Registration of ultrasound images is often complicated due to inherent noise. Robust similarity metrics and optimization procedures are required to facilitate medical applicability. In this paper a novel hybrid procedure, incorporating global statistics and local textural features, is proposed for the registration of envelope detected radio frequency ultrasound data. On the global scale this is achieved by Hellinger distance between distribution in images, and on the local scale by a statistics-based extension of Fuzzy Local Binary Patterns (FLBP). The proposed procedure is shown to outperform standard measures such as SSD and NCC, as well as Hellinger distance and histogram matching of standard FLBPs, in rigid registration experiments of envelope detected radio frequency data samples of the human neck.

***Index Terms*—** Ultrasound, Radio Frequency (RF), Similarity, Hellinger, Local Binary Patterns, Nakagami

1. INTRODUCTION

Registration of images is a fundamental problem in several fields, particularly in the domain of medical imaging. However, issues such as noise and artifacts complicate this process and often make automatic registration processes intractable. Those issues are in particular prevalent in ultrasound (US) imaging due to its complex physical nature. Nevertheless, there exist a multitude of applications in US registration such as in elastography, speckle tracking and motion recovery. Hence, the development of similarity metrics in US registration is an active field of research. A common approach in modeling this problem is to employ statistical methods. Unlike in the conventional vision domain, where the Gaussian intensity distribution has been successfully applied in a variety scenarios, in US other models are more appropriate. This is particularly the case for envelope detected radio frequency (RF) US data. The statistical properties of the echo envelope of US data depend on numerous factors. Among them is, in particular, the density and spatial distribution of scatterers in the medium. As different types of biological tissue exhibit various characteristics w.r.t. density and scatterer distribution, this can be utilized for registration purposes. Given enveloped RF data, the following models have been proposed. For fully developed speckle the Rayleigh distribution [1] applies. The Rice distribution has been suggested [1, 2] for the case of coherent, or structured, high density scatterers, while for partially developed speckle, the K-distribution [3, 4] has been shown to be appropriate. Moreover, general models have been proposed in the literature such as the generalized K-distribution and the homodyned K-distribution (see e.g., [3] and [5]) and most recently the Rician Inverse of Gaussian distribution [6]. These models can account for a multitude of scattering conditions, however at the price of high analytical complexity. Comparatively simpler, but nevertheless versatile, the Nakagami distribution [7, 8] can account for varying scattering conditions, and so is the method of choice in this paper.

This work was partly sponsored by EU grant FP7-ICT-2009-6-270460

2. METHOD

Given the noisy nature of US, using statistical measures for the sake of robustness seems evident. In order to improve the registration accuracy a hybrid approach is proposed that couples the global concept of distribution matching with a local one measuring texture patterns. We refer to this in the following as hybrid local binary pattern (HLBP). The two components of HLBP are based on the Gamma Hellinger distance metric, cf. Sec. 2.1, and Local Binary Patterns, cf. Sec. 2.2, resp. Additionally, we make use of US confidence maps for parameter estimation.

2.1. Gamma Hellinger distance metric

We use the Nakagami distribution [7, 8] for modeling the speckle distribution in envelope detected RF US data. The Nakagami distribution is closely related to the Gamma distribution, and so may be used in its stead, by application of a simple transformation of data, specifically

$$\begin{aligned} \text{if} \quad Y \sim f_{gam}(x \mid m,k) \quad \text{and} \quad & X \sim f_{nak}(x \mid \mu,\omega) \\ \text{then} \quad & \sqrt{X} = Y(\mu, \frac{\omega}{\mu}) \ , \end{aligned} \tag{1}$$

where f_{gam} and f_{nak} denotes the Gamma and Nakagami PDF, resp.

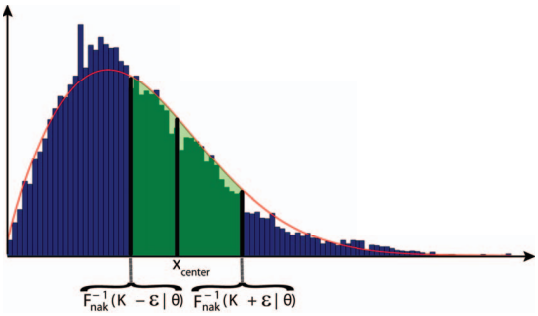


Fig. 1. The threshold parameter ϵ defining a probability interval around the central site intensity value.

One option in distribution matching is the Hellinger distance metric. The Hellinger distance H_{gam} between two probability Gamma distributions F and G, is expressed by their associated density functions $f \sim f_{\text{gam}}(x|m_1, k_1)$ and $h \sim f_{\text{gam}}(x|m_2, k_2)$ as

$$H_{gam}(f,h) = 1 - \frac{\Gamma\left(\frac{(m_1+m_2)}{2}\right)}{\left[\Gamma(m_1)\Gamma(m_2)\right]^{\frac{1}{2}}} \cdot \frac{\left(\frac{(k_1+k_2)}{2}\right)^{-\left(\frac{m_1+m_2}{2}\right)}}{\left[\frac{1}{k_1{}^{m_1}} \cdot \frac{1}{k_2{}^{m_2}}\right]^{\frac{1}{2}}}, \tag{2}$$

with $H_{gam}(f,h) \in [0,1]$. We apply Hellinger distance alone and in conjunction with Local Binary Patterns, cf. Sec. 2.5, in registration of envelope detected US data, which to our knowledge, is a novel approach.

2.2. Local Binary Pattern

Texture classification is a wide domain in which numerous approaches exist. A relatively simple, but powerful and popular technique in computer vision, are the so called local binary patterns (LBP), which were originally introduced by Ojala *et al.*in [9]. In its standard formulation it encodes a second order neighborhood of a pixel into a 2^8 bits code. Encoding is based on the inequality relationship between the central site intensity and its 8 neighbors. A pixel position with lower intensity than the central one is attributed the binary code 0, otherwise 1. From those individual binary digits a code for the neighborhood and finally a histogram of codes, serving as descriptor for a region, is built. Given that the origin of LBPs lies in computer vision, their application is mainly tailored to natural scene images. However, there also exist adaptations to cope with images that are inherently subject to noise. Iakovidis *et al.*[10] proposed FLBP for US, in which not only a single LBP but various codes can represent a region, therefore being more robust in noisy image domains. A threshold specifies an intensity range in which fuzziness is assumed and a ramp (membership function) associates the probability for the binary class encoding. For measuring similarity between LBP histograms, several methods have been proposed such as Histogram intersection, Log-likelihood statistic and Chi-square statistic - see [11] for a comparative study.

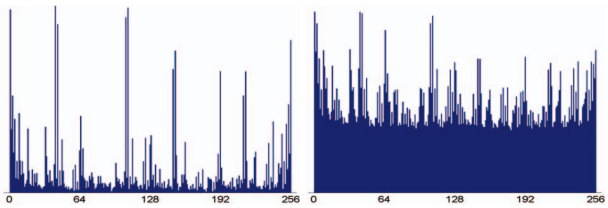


Fig. 2. Feature histograms for low (*left*) and high (*right*) threshold.

2.3. Statistics-based Membership Function

Unlike the original FLBP [10], which defines the membership function as a ramp, we propose a non-linear function associated with the underlying statistical properties of data. Let

$$f_{\text{nak}}(x \mid \mu, \omega) = \frac{2\mu^{\mu} x^{2\mu-1}}{\Gamma(\mu)\omega^{\mu}} \exp\left(-\frac{\mu}{\omega}x^2\right), \forall x \in \mathbb{R}_+ \tag{3}$$

be the PDF of the Nakagami distribution with μ, ω the shape and scale parameters, resp. Its corresponding CDF is

$$F_{\text{nak}}(x \mid \theta) = \frac{\gamma(\mu, \frac{\mu}{\omega}x^2)}{\Gamma(\mu)}, \tag{4}$$

with $\theta = \{\mu, \omega\}$ and γ being the incomplete gamma function. Following the idea of FLBP, a membership function $m_j(x)$ is defined, denoting the confidence of a class association $j \in \{0,1\}$ given intensity x. Membership symmetry is assumed, i.e. $m_0(x) = 1 - m_1(x)$. However, as opposed to to FLBP, the membership function m_1 is non-linear, given by

$$m_1(x_i) = \begin{cases} 1, & x_i > F^{-1}_{\text{nak}}(K+\epsilon|\theta), \\ \frac{F_{\text{nak}}(x_i|\theta)-K}{2\epsilon} + \frac{1}{2}, & x_i \in (x_{\text{cntr}}, F^{-1}_{\text{nak}}(K+\epsilon|\theta)] \\ \frac{K-F_{\text{nak}}(x_i|\theta)}{2\epsilon}, & x_i \in [F^{-1}_{\text{nak}}(K-\epsilon|\theta)), x_{\text{cntr}}] \\ 0, & x_i < F^{-1}_{\text{nak}}(K-\epsilon|\theta) \end{cases} \tag{5}$$

where $K = F_{\text{nak}}(x_{\text{cntr}}|\theta)$, and x_{cntr} and x_{i} denotes the intensity at the center site and site i, corresp. In the fuzzy region $[F^{-1}_{\text{nak}}(K-\epsilon|\theta), F^{-1}_{\text{nak}}(K+\epsilon|\theta)]$, as illustrated in Fig. 1, the membership function is the normalized cumulative within class probability. As ϵ increases, more fuzziness is assumed, and thus more noise is compensated for. Generally, the influence of ϵ is quite data dependent. One possibility is to define it as a combination of a probability threshold T with a confidence value C, s.t $\epsilon = T \cdot C$. Here we employ a Confidence Map (see Sec. 2.4) corresp. to the US image, to approximate C. The underlying idea is that low confidence regions should be compensated in terms of increased fuzzyness. See Fig. 2 for a visualization how the magnitude of the threshold ϵ affects the feature histogram.

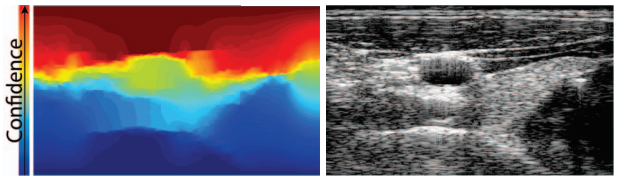


Fig. 3. Confidence map (left) and the corresp. RF image (right).

2.4. Confidence Maps

We formulate the US signal confidence estimation as a random walk problem. The solution to this is based on the algorithm proposed for image segmentation [12]. There a multi-label image segmentation is obtained by the analytic computation of the probabilities for random walks reaching user-defined image labels. For the confidence estimation we are interested in the probabilities of random walks reaching the transducer elements under US specific constraints. More specifically, the random walks behavior is adjusted by modifying the graph Laplacian [13] to model US transmission, beam-width, and depth-dependent attenuation. Subsequently, the analytic solution expresses the probability of US energy reaching a point in the RF data domain. In [13] confidence maps are computed for Intravascular Ultrasound RF to emphasize uncertainty and detect lack of acoustic energy in regions of interest. In this work they are utilized for a different application, namely, the definition of a new similarity measure for mono-modal US registration.

2.5. Hybrid Similarity Measure

A common approach to measuring the similarity between LBPs is histogram intersection

$$D_{X,Y} = \sum_i min(X_i, Y_i) \; . \tag{6}$$

However, standard histogram intersection is prone to yield several local minima. In order to avoid this, we endow the standard histogram intersection with a component measuring the statistical similarity of distributions. This follows the notion that patterns, in the two patches of intensities being considered, should be considered as relevant where the underlying distributions significantly exhibit high similarity. Statistical similarity alone on the other hand is globally precise (*rough scale*), but is locally (*fine scale*) imprecise. However, in combination with, the in Sec. 2.3 proposed statistics-based FLBP, which has diametrically opposite behaviour, i.e. globally imprecise and locally precise (see Fig. 6), we yield overall high reliability. The hybrid Hellinger weighted histogram intersection is defined as

$$D_{\text{Hybrid}} = D_{X,Y} \cdot \exp(-\Delta \bar{H}_{gam}(f,h)) + \bar{H}_{gam}(f,h), \tag{7}$$

where Δ denotes the influence radius of the patch-averaged distribution distance $\bar{H}_{gam}$, which implies multiple Hellinger

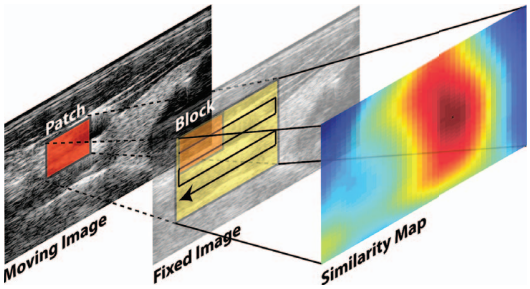


Fig. 4. Concept of block matching and derivation of the similarity maps.

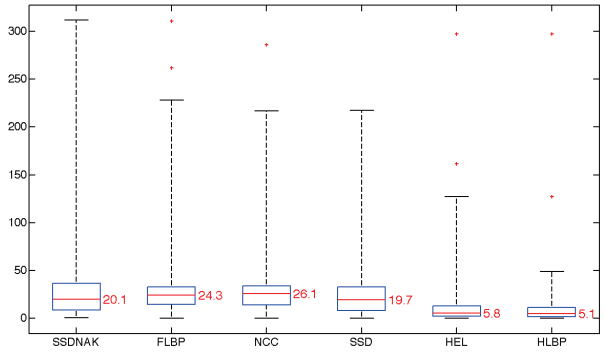


Fig. 5. Global registration performance for all datasets combined - error measured in pixels.

distance computations on corresponding (homogenous) subpatches. Furthermore X, Y contain the LBP feature histograms (see Sec. 2.3). This reinforces the notion that LBP is primarily used to enhance the accuracy of Hellinger, which determines a robust rough approximation of the location of the global optima.

3. EXPERIMENTS

Experiments are performed on 5 human neck datasets each acquired with a 10 MHz linear array probe yielding RF envelope images of size 2048 x 256 pixels. Images were recorded with an Ultrasonix MDP machine. The registration dataset consists of pairs of images constituting a moving and a fixed image for the registration (translation, 2 degrees of freedom). Consequently, block matching (block size 20 x 40 pixels) is performed at 28 regular spaced points on the image domain, yielding similarity maps. See Fig. 4 for a schematic visualization of the block matching process. For each block 20 registration runs are performed with random initial start points to estimate the susceptibility of metrics towards building local minima. Manual alignment of each dataset pair served as ground truth. The following methods were used for the registration test: SSD (Sum-Of-Squared Differences), SSDNAK (SSD on the shape parameter of Nakagami images), NCC (Normalized Cross-Correlation), FLBP (threshold $\epsilon = 30$,

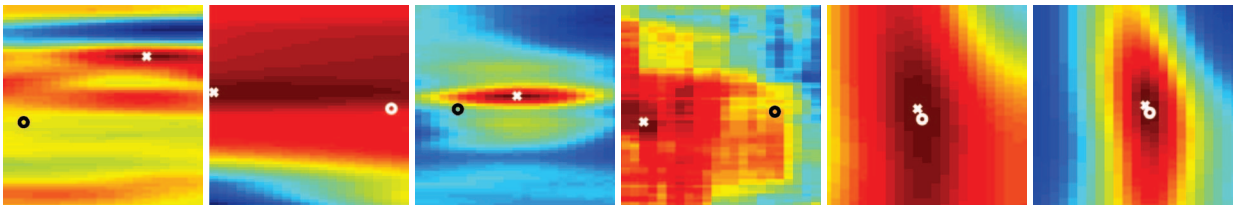


Fig. 6. Similarity maps from left to right: SSD, SSDNAK, NCC, FLBP, HEL and HLBP. Circle: ground truth optimum; Cross: optimum in similarity map.

Dataset	SSD	SSDNAK	NCC	FLBP	HEL	HLBP
#1	20.1	23.0	26.1	28.1	4.7	**3.5**
#2	16.1	19.8	26.3	28.2	7.4	**6.3**
#3	20.1	12.1	26.2	27.2	7.9	**7.4**
#4	17.9	16.5	25.0	24.0	8.5	**7.4**
#5	24.4	19.9	27.2	3.3	1.4	**1.3**

Table 1. Median errors (pixels) of random registration study for various datasets and similarity metrics.

confidence weighted), Hellinger and HLBP (threshold $\epsilon = 0.35$, confidence weighted). Finally, the global similarity is computed by accumulating estimates from all blocks on each dataset - see Table 1 for median pixel errors. For registration performance evaluation, comparison results from all datasets are combined - see Fig. 5. Additionally, in order to assess the different similarity measures we extract a patch in the moving image, and compute corresp. similarity maps - see Fig. 6 for an example.

4. CONCLUSION

In this paper the novel similarity metrics Nakagami Hellinger and HLBP were proposed. Results of the experiments show that HLBP greatly outperforms standard methods, such SSD and NCC, and also improves upon the result obtained by use of Hellinger distance metric. The robustness of HLBP is due to its hybrid local and global strategy. On the one hand, LBP and its variants are able to take into account very fine textural features in data, which can discriminate small local differences between images, and are thus suitable for small-scale alignments. On the other hand, when differences are large between images, fine textural differences are not relevant. Here a purely statistical (dis-)similarity measure like e.g. Hellinger distance, is a better candidate for detecting global differences between images. For future work, optimization of the neighborhood system of HLBP will be investigated, as this has been shown in initial experiments to be a source of potential major improvement.

5. REFERENCES

[1] Robert F. Wagner, Stephen W. Smith, John M. Sandrik, and Hector Lopez, "Statistics of Speckle in Ultrasound B-Scans," *IEEE Trans. Sonics Ultrason.*, vol. 30, no. 3, pp. 156–163, 1983.

[2] M.F Insana and et al., "Analysis of ultrasound image texture via generalized rician statistics," *Opt. Eng*, vol. 6, no. 4-5, pp. 743–748, 1986.

[3] E. Jakeman, "K-distributed noise," *J. Opt. A: Pure Appl. Opt*, vol. 1, no. 4-5, 1999.

[4] P.M. Shankar and et al., "Use of non-rayleigh statistics for the identification of tumors in ultrasonic b-scans of the breast," *TMI*, vol. 12, no. 4-5, pp. 687–692, 1993.

[5] V Dutt and et al., "Ultrasound echo envelope analysis using a homodyned k-distribution signal model," *Ultrason. Imag.*, vol. 16, no. 4-5, pp. 265–287, 1994.

[6] T. Eltoft, "Speckle: Modeling and filtering," in *Norwegian Signal Process. Symp.*, October 2-3 2003.

[7] P.M. Shankar, "A general statistical model for ultrasonic scattering from tissues," *T-UFFC*, vol. 47, no. 3, pp. 339–343, Mar 2000.

[8] N. Nakagami, "The m-distribution, a general formula for intensity distribution of rapid fadings," in *Statistical Methods in Radio Wave Propagation*, W. G. Hoffman, Ed. Oxford, England: Pergamon, 1960.

[9] T Ojala and et al., "Multiresolution gray-scale and rotation invariant texture classification with local binary patterns," *T-PAMI*, vol. 24, no. 7, pp. 971–987, 2002.

[10] D. K Iakovidis and et al., "Fusion of fuzzy statistical distributions for classification of thyroid ultrasound patterns," *Artif. Intell. Med.*, vol. 50, pp. 33–41, 2010.

[11] Jukka Ahonen and et al., "Face Recognition with Local Binary Patterns," pp. 469–481. ECCV, 2004.

[12] L. Grady, "Random walks for image segmentation," *T-PAMI*, vol. 28, pp. 1768–1783, 2006.

[13] Karamalis et al., "Confidence estimation in IVUS radiofrequency data with random walks," in *ISBI*, 2012.